

高耐磨药芯焊丝堆焊组织及基体选择

李 达¹, 杨庆祥¹, 崔占全¹, 杨育林^{2*}

(1. 燕山大学 亚稳材料制备技术与科学国家重点实验室, 河北 秦皇岛 066004;
2. 燕山大学 机械工程学院, 河北 秦皇岛 066004)

摘 要: 制备了高铬铸铁型自保护药芯焊丝, 并采用此焊丝分别在 Y-Ni4 铸铁、65Mn 钢、40Cr 钢和灰口铸铁基体上进行堆焊。对不同堆焊试样进行硬度测试, 对堆焊金属及其结合部位进行显微组织及断口形貌观察。结果表明, 堆焊金属硬度在 60HRC 以上, 断裂方式均为解理断裂。65Mn 钢堆焊试样熔合较好, 且基本无裂纹, 可在受冲击载荷较大的条件下使用; Y-Ni4 铸铁堆焊试样熔合良好, 但在热影响区存在裂纹, 应在冲击载荷较小或不受冲击载荷条件下使用; 40Cr 和灰铸铁堆焊试样熔合不好, 熔合区存在许多缺陷, 不宜作为耐磨堆焊基体材料。

关键词: 药芯焊丝; 堆焊金属; 结合部位; 显微组织

中图分类号: TG422.3 文献标识码: A 文章编号: 0253-360X(2009)12-0069-04



李 达

0 序 言

磨辊、磨盘等许多耐磨零件在使用一段时间后都会因为表面磨损而失效^[1,2]。目前, 通常采用药芯焊丝堆焊的方法修复这些失效的零件。耐磨堆焊技术广泛应用于矿山、机械、电力及冶金等行业中的一些零件上, 比如水泥工业中的辊压机挤压辊、风机叶片、破碎机滚筒、衬板、锤头、磨煤机辊套、磨球、立磨磨辊及磨盘等^[3-5]。

许多耐磨零件如果采用整体一种材料铸造, 不仅制造困难, 而且造价昂贵。另外, 许多耐磨零件如立磨磨辊磨损到一定尺寸后整个零件就会失效, 虽然可以采用堆焊方法修复, 但也只能修复 2~3 次, 而且辊体本身脆性较大, 容易出现整个辊体断裂^[6]。目前, 在制造大型立磨磨辊及磨盘时经常采用复合耐磨堆焊再制造的方法, 即辊体基体采用韧性良好、价格低廉、表面堆焊高硬度高耐磨材料, 以达到内部具有足够韧性, 而表面具有较高耐磨性的复合工作层。再制造的耐磨零件要具有较好的综合力学性能, 因此, 合理的选择基体材料具有重要的意义。

高铬铸铁型药芯焊丝堆焊组织一般由马氏体、M₇C₃ 型碳化物及残余奥氏体构成, 其堆焊层表面具

有较高的硬度和耐磨性^[7-9]。文中自行研制了高铬铸铁型药芯焊丝, 并采用该焊丝分别在 Y-Ni4 铸铁、65Mn 钢、40Cr 钢和灰口铸铁四种基体上进行堆焊, 分析堆焊层组织及析出相以及不同基体与堆焊层的结合情况, 为实际大型耐磨零部件堆焊再制造时选择基体提供依据。

1 试验方法

药芯焊丝制作过程采用 H08A 薄钢带作为外皮, 药芯中分别添加高碳铬铁、高碳锰铁、硅铁、片状石墨以及钒铁等合金粉末。分别选用 Y-Ni4 铸铁、65Mn 钢、40Cr 钢、灰口铸铁作为基体试样, 利用 YM600KH 型焊机进行手工堆焊, 焊接工艺参数见表 1。

表 1 焊接工艺参数
Table 1 Welding parameters

焊接电流 <i>I</i> /A	焊丝直径 <i>D</i> /mm	电源 极性	焊丝伸出长度 <i>l</i> /mm	电弧电压 <i>U</i> /V
250~400	3.2	直流反接	25~30	28~35

在不同堆焊试样上用线切割切取小块试样分别记为 A1, A2, A3, A4 进行试验。将制好的小块试样用金相砂纸磨平, 抛光后用 4% 硝酸酒精溶液进行腐蚀, 在 XJG-05 金相显微镜下对各堆焊试样的堆焊

收稿日期: 2008-08-07
基金项目: 河北省科技攻关资助项目(04212201D); 河北省百名优秀
人才支持计划资助项目(09215106D)。
* 参加此项研究工作的还有翁露露。

金属及结合部位进行显微组织观察. 采用 $D_{\max} - 2500$ PC X 射线衍射仪对 Y-Ni4 铸铁堆焊金属中的析出相进行分析, 在扫描电镜 KYKY2800 下观察各基体的断口形貌及裂纹情况, 通过分析选择合适的基体材料.

2 试验结果与分析

2.1 药芯焊丝堆焊金属

2.1.1 堆焊金属成分分析

对自制药芯焊丝堆焊金属化学成分进行分析, 结果见表 2.

表 2 堆焊金属化学成分(质量分数, %)
Table 2 Composition of hardfacing metal

Cr	C	Si	Mn	Ni	Fe
25	4	2	1.5	1.5	余量

2.1.2 硬度分析

在 HR-150A 型洛氏硬度计上对各试样堆焊金属侧面进行硬度分析, 结果见图 1.

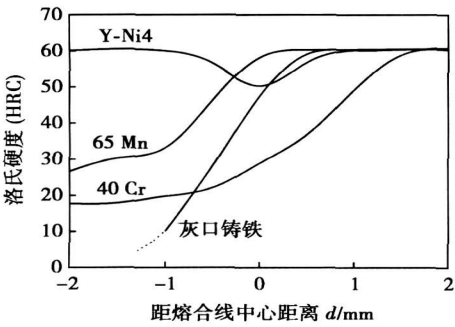


图 1 堆焊金属侧面硬度分布

Fig. 1 Hardness distribution of hardfacing metals

由图 1 可知, 堆焊金属硬度达到 60 HRC 以上. 各种基体中, Y-Ni4 铸铁硬度是最高的, 但在熔合区附近其硬度有所降低, 这可能与焊接时的回火软化有关. 在二次加热情况下, 过饱和的碳将向晶界扩散, 并与铬形成碳化物沉淀于晶界, 使晶粒内部的铬产生“供不应求”现象, 从而导致靠近晶界的薄层严重缺铬. 从图 1 中还可看出, 灰口铸铁、40Cr 钢和 65Mn 钢的硬度从母材到堆焊层呈上升趋势.

2.1.3 堆焊层显微组织

图 2 为高铬铸铁型药芯焊丝堆焊金属显微组织形貌, 由图 2 中可以看出堆焊金属组织主要为马氏

体基体及白色的 M_7C_3 碳化物, 其中碳化物呈孤立的块状, 均匀分布在基体中, 这样的组织使堆焊层具有较高的硬度及耐磨性.

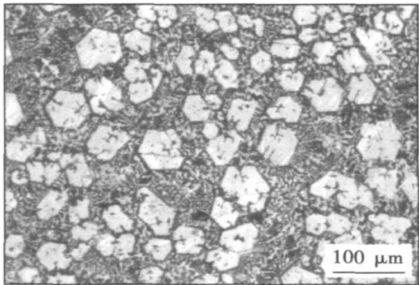


图 2 堆焊金属金相组织形貌

Fig. 2 Microstructure of hardfacing metals

2.1.4 X 射线衍射分析

图 3 为堆焊金属的 X 射线衍射分析结果, 结合显微组织照片可以看出, 堆焊金属中主要为 M_7C_3 型碳化物、马氏体以及少量残余奥氏体.

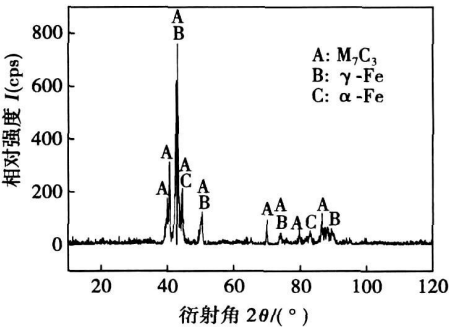


图 3 堆焊金属 X 射线衍射图谱

Fig. 3 X-ray diffraction analysis of hardfacing metal

2.2 结合部位观察

2.2.1 显微组织观察

分别在金相显微镜下对 4 种试样进行组织观察, 其熔合区组织分布见图 4, 各图下半部分为堆焊金属. 热影响区附近组织形貌见图 5.

从图 4 中可以看出 Y-Ni4 铸铁基体与堆焊金属结合最好, 但从图 5 中可以看出 Y-Ni4 铸铁基体在焊接过程中热影响区出现裂纹; 65Mn 钢与堆焊金属结合情况较好, 热影响区附近没有明显裂纹, 其组织有些粗化, 但可以通过控制焊接工艺以及利用热处理来改善; 40Cr 钢和堆焊金属熔合较差, 因为两者成分相差比较大; 灰口铸铁熔合情况一般, 由于灰口铸铁本身含有大量的片状石墨及本身碳当量较高,

可焊性不好, 熔合区出现大量气孔。

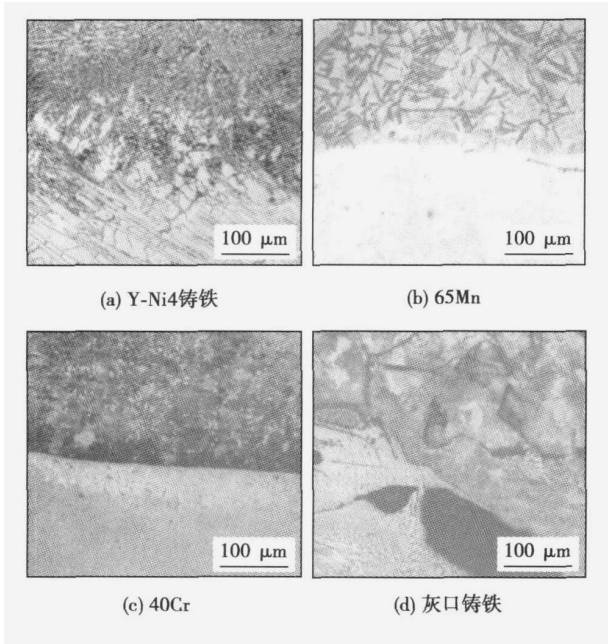


图 4 不同堆焊试样熔合区组织形貌

Fig. 4 Microstructures of binding zone of different hardfacing specimens

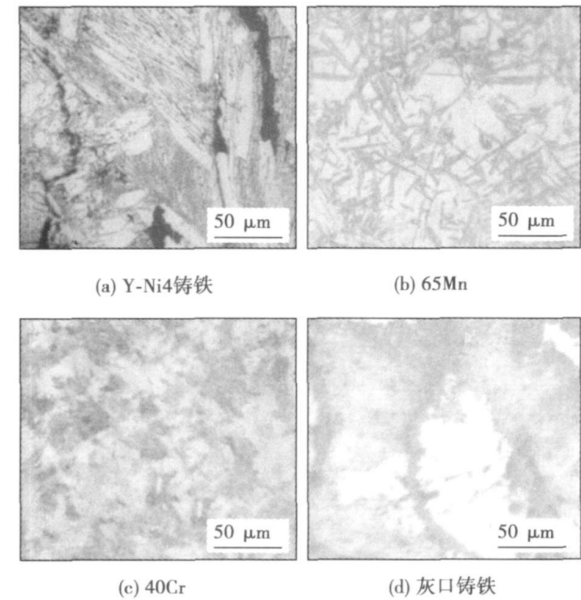


图 5 不同堆焊试样热影响区附近组织形貌

Fig. 5 Microstructures near heat affected zone of different hardfacing specimens

2.2.2 SEM 断口分析

将 4 种堆焊试样在室温下冲断, 然后通过扫描电镜观察其断口形貌, 如图 6 所示。图中上半部分均为堆焊金属, 下半部分为基体。

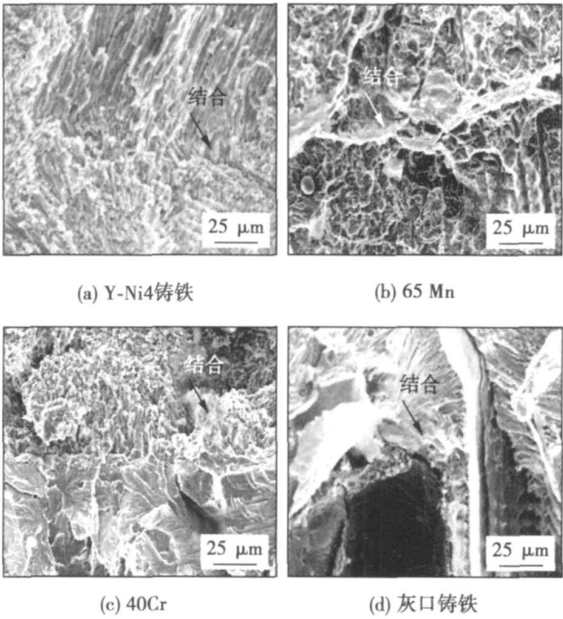


图 6 高倍下各堆焊金属断口宏观形貌

Fig. 6 Fracture morphology of different hardfacing metal

从图 6a 中可见 Y-Ni4 铸铁堆焊试样断口较为平滑, 熔合区结合得比较好, 没有明显的熔合线。其断裂方式主要为解理断裂, 且堆焊金属、熔合区及基体都有较多裂纹存在。从图 6b 可见 65Mn 钢与堆焊金属结合不如 Y-Ni4 铸铁, 但 65Mn 钢基体主要是以韧窝状断裂为主, 伴有准解理断裂, 韧性较 Y-Ni4 铸铁要好, 在熔合区没有明显的裂纹及其它缺陷。从图 6c 可见 40Cr 钢基体和堆焊金属断裂方式明显有差别, 基体为韧窝状断裂, 伴有准解理断裂。而堆焊金属是解理断裂且熔合区比较窄, 在堆焊金属熔合区和基体上存在着一些裂纹。从图 6d 可见灰口铸铁基体和堆焊金属都较脆, 断裂方式主要是解理状, 且熔合区比较疏松, 气孔较多。

3 讨 论

由上述试验及分析可知, 各种基体中以 Y-Ni4 铸铁为基体的堆焊金属及基体硬度较高, 与药芯焊丝较匹配, 熔合情况最好, 但熔合区和基体出现大量裂纹不利于实际工作条件, 特别是在有冲击力的情况下。

65Mn 钢为基体的堆焊金属硬度达到要求, 熔合情况比较好, 熔合区、母材并没有像 Y-Ni4 铸铁那样出现裂纹, 但母材硬度较 Y-Ni4 铸铁低, 可知 65Mn 钢基体塑性、韧性比较好, 与高硬度的堆焊金属结合较好, 故在工作条件下特别是有较小冲击的情况下使用情况比较好。

40Cr 钢为基体的堆焊金属其基体硬度比较低,不利于实际工作. 同时 40Cr 钢与堆焊金属结合情况不够好, 并且基体及堆焊金属及其交界处有裂纹产生不利于实际工作. 由于堆焊层的硬质相硬度比基体要高出很多, 因而在磨料磨损的切向应力作用下, 在硬质相与基体之间的界面区, 容易产生位错塞积和较大的塑性变形, 当应力值达到某一临界值时, 将导致裂纹的萌生和扩展, 使硬质相从基体剥落导致磨损.

灰口铸铁为基体的堆焊金属其基体硬度更低($< 15\text{ HRC}$), 不适于实际工作, 同时结合情况亦比较差, 夹杂、气孔及裂纹比较多, 因此可知其焊接性较差, 不适于实际再制造中的基体材料.

由上述讨论可知, 比较适合用于磨辊的基体为 Y-Ni4 铸铁与 65Mn 钢. 在无冲击或冲击力不大的情况下选用 Y-Ni4 铸铁比较好, 但是在冲击力较大的情况下可以使用 65Mn 钢替代 Y-Ni4 铸铁.

4 结 论

(1) 高铬铸铁型药芯焊丝堆焊金属硬度在 60 HRC 以上, 堆焊金属组织主要为马氏体及 M_7C_3 型碳化物.

(2) 由金相及扫描结果可知, Y-Ni4 铸铁作为基体时, 熔合较好, 堆焊层和基体硬度都较高, 但热影响区存在裂纹, 所以适合应用在抗冲击力小的耐磨场合; 65Mn 钢作为基体时, 熔合较好, 且基体不存在裂纹, 而 65Mn 钢基体韧性比较好, 因此可用在表面要求耐磨, 而内部要有足够韧性的场合.

参考文献:

[1] 梁志刚, 白晓军, 王智磊. 在线耐磨堆焊技术在 RP-1043 磨煤机的应用[J]. 科学之友(B 版), 2007(2): 13-15.
Liang Zhigang, Bai Xiaojun, Wang Zhilei. The application of on-Line wear resisting welding technique in RP-1043 coal mill[J]. Friend of Science Amateurs (Edition B), 2007(2): 13-15.

[2] 张昆谋, 郑国良, 彭新桥. 浅谈立磨磨辊及磨盘表面耐磨堆焊技术[J]. 新世纪水泥导报, 2005, 11(6): 47-48.
Zhang Kunmou, Zheng Guoliang, Peng Xinqiao. Brief analysis of the wearable surface welding technology on roller mill and grinding disc[J]. New Century Cement Review, 2005, 11(6): 47-48.
[3] 扬威, 王欣, 张永生, 等. 高铬铸铁耐磨堆焊埋弧药芯焊丝的研究[J]. 中国表面工程, 2007, 20(4): 33-37.
Yang Wei, Wang Xin, Zhang Yongsheng, et al. The research of hardfacing submerged flux-cored wires with high Cr cast iron[J]. China Surface Engineering, 2007, 20(4): 33-37.
[4] 黄智泉, 魏建军, 潘健. 堆焊用药芯焊丝的发展及其应用前景[J]. 机械工人: 热加工, 2004(8): 38-40, 44.
Huang Zhiquan, Wei Jianjun, Pan Jian. The development and application of the flux-cored wire in surfacing area[J]. Machinist Metal Forming, 2004(8): 38-40, 44.
[5] 胡邦喜, 莽克伦, 王静洁, 等. 堆焊技术在国内石化、冶金行业机械设备维修中的应用[J]. 中国表面工程, 2006, 19(3): 4-8.
Hu Bangxi, Mang Kelun, Wang Jingjie, et al. Application of surfacing on mechanism equipments maintaining of petroleum chemical industry and metallurgy industry in China[J]. China Surface Engineering, 2006, 19(3): 4-8.
[6] 魏建军, 潘健, 黄智泉, 等. 耐磨堆焊材料在我国水泥工业中的应用[J]. 中国表面工程, 2006, 19(3): 9-13.
Wei Jianjun, Pan Jian, Huang Zhiquan, et al. The application of hardfacing material in chinese cement industry[J]. China Surface Engineering, 2006, 19(3): 9-13.
[7] Buchanan V E, McCartney D G, Shipway P H. A comparison of the abrasive wear behaviour of iron-chromium based hardfaced coatings deposited by SMAW and electric arc spraying[J]. Wear, 2008, 264(7-8): 542-549.
[8] Fan C, Chen M, Chang C M, et al. Microstructure change caused by $(Cr, Fe)_{23}C_6$ carbides in high chromium Fe-Cr-C hardfacing alloys[J]. Surface and Coating Technology, 2006, 201(3-4): 908-912.
[9] 王清宝, 王智慧, 李世敏. Fe-Cr-C 系高碳耐磨堆焊合金组织及性能[J]. 焊接学报, 2004, 25(6): 119-123.
Wang Qingbao, Wang Zhihui, Li Shimin. Microstructures and properties of Fe-Cr-C hardfacing alloys with high carbon content[J]. Transactions of the China Welding Institution, 2004, 25(6): 119-123.

作者简介: 李 达, 男, 1982 年出生, 博士研究生. 主要从事焊接材料的研制及焊接模拟方面的工作. 发表论文 10 篇.

Email: y. yang@ysu.edu.cn

Key words: TIG welding; weld pool shape; turbulent flow; numerical simulation

Calibration approach for structured-light sensor in remanufacture based on welding robot YIN Ziqiang, ZHANG Guangjun, GAO Hongming, WU Lin (State Key Laboratory of Advanced Welding Production Technology, Harbin Institute of Technology, Harbin 150001, China). p 57—60

Abstract On the flexible remanufacture platform based on welding robot, 3D ranging of the damage parts is the key step to obtain the remanufacturing data. This paper proposes a rapid calibration approach and calibrates the line structured-light 3D ranging system in the flexible remanufacture platform of the welding robot. The calibration includes the following steps: first, calibrates internal and external parameters of the camera by a planar pattern; second, solves parameters of the light plane by the structured-light strip in the image, which determine the relationship between light plane and camera; and then calculate 3D coordinate of the feature point on the damage parts to establish remanufacture model. The approach is easy, simple and accurate.

Key words: welding robot; remanufacture; structured-light; calibration

Flash butt welding of bainite steel crossing with U71Mn steel rail

WANG Xin, ZHANG Fucheng, LÜ Bo, ZHENG Chunlei (State Key Laboratory of Metastable Materials Science and Technology, Yanshan University, Qinhuangdao 066004, China). p 61—64

Abstract: The temperature field distribution of heat-affected zone (HAZ) in weld joints of bainite steel and U71Mn steel and the technical parameters of upset pressure of flash butt welding were determined by using the Gleeble thermal simulation test technology. After some small specimens of bainitic crossing steel and U71Mn rail steel were welded with a miniature flash butt welder by using the results of the parameters to determine the technical parameters of flash butt welding experiment, bainitic steel crossing and U71Mn steel rail were practically welded with Gaas-100 direct current flash butt welder. The mechanical properties, including tensile toughness, impact test and hardness and the microstructure of welded joints were analyzed. The results show that the best upset pressure of flash butt welding is about 30 MPa, which the HAZ is very small, and the mechanical properties of the welded joint comes up to the standard of the Ministry of Railway. The welding bainitic crossing steel and U71Mn rail steel by flash butt welding is completely feasible.

Key words: crossing; welding; bainite steel

Analysis on the thermal fatigue behavior of QFP soldered joints

SHENG Zhong, XUE Songbai, ZHANG Liang, GAO Lili (College of Materials Science and Technology, Nanjing University of Aeronautics and Astronautics, Nanjing 210016, China). p 65—68, 104

Abstract: The creep strain and plastic strain of soldered joints in time history are studied and analyzed with numerical simulation method, which are found to be accumulated as ladder form.

Based on Solomon and Shine and Fox models, the fatigue life values of the Sn-Pb and SnAgCu soldered joints are evaluated by equivalent strain, which are about 937 and 1 391 respectively. The experimental results showed both in experiment and simulation results indicate that the tensile force of soldered joints will be decreased with the increase of thermal cycling times, the reliability of SnAgCu after thermal cycling is better than that of Sn-Pb, the fracture mode of the soldered joints transforms from toughness fracture into brittle fracture, and the brittle intermetallic compounds at the interface of soldered joints will grow up gradually with the increase of thermal cycling times during thermal cycling process, which give a strong impact to the reliability of soldered joints and reduce the tensile force of soldered joints at the same time.

Key words: numerical simulation method; fatigue life; tensile force; intermetallic compound

Microstructure of hardfacing metal and matrix materials with high abrasive flux-cored wire LI Da¹, YANG Qingxiang¹,

CUI Zhanquan¹, YANG Yulin² (1. State Key Laboratory of Metastable Materials Science & Technology, Yanshan University, Qinhuangdao 066004, China; 2. School of Mechanical Engineering, Yanshan University, Qinhuangdao 066004, China). p 69—72

Abstract Four matrix materials, Y-Ni4 cast iron, 65Mn steel, 40Cr steel and grey cast iron, were hardfaced by the high chromium cast iron of self-shielded flux-cored wire separately. The hardness of different hardfacing specimens was measured, and the microstructures, fracture morphologies and the binding sites of different hardfacing specimens were observed. The results show that the hardness of the hardfacing metal is over 60 HRC and the fracture is of cleavage type. The fusion zones of 65Mn and Y-Ni4 hardfacing metal are good ones. However, the cracks can be observed in the heat-affected zone of Y-Ni4 hardfacing specimen. Therefore, the hardfacing metal of 65Mn steel is suitable for the condition of high stress wear and Y-Ni4 cast iron is suitable for the lower one. Besides, there are many defects in the fusion zone of 40Cr and grey cast iron hardfacing specimens, which are not suitable for the wear resistant matrix materials.

Key words: flux-cored wire; hardfacing metal; binding sites; microstructure

Exploring blowhole resistance of new slag system stainless steel electrode by uniform design method MENG Gongge¹, YANG

Deyun², LI Dan¹ (1. School of Material Science & Engineering, Harbin University of Science and Technology, Harbin 150040, China; 2. Huade School of Applied Technology, Harbin Institute of Technology, Harbin 150025, China). p 73—76

Abstract After analyzing some domestic and abroad electrode coating systems, a new slag system of stainless steel electrode was designed. The experiment was arranged by uniform design method and computer program. 11 coating components, each of them being divided into 10 levels, were selected as independent variables, and 30 tests were done in all. The statistical data analysis was done